Available online at www.sciencedirect.com

ScienceDirect

Procedia Engineering 10 (2011) 1709–1717

Engineering Procedia

ICM11

Percolation and Film Formation Behaviors of MWNT/PS Nanocomposites

S. Ugur[a]*, O. Yargi[b] and O. Pekcan[c]

[a,b]*Department of Physics Istanbul Technical University, Maslak 34469, Istanbul TURKEY*
[c]*Kadir Has University, Cibali 34320, Istanbul TURKEY*

ABSTRACT

This study involves the investigation of film formation and electrical conductivity properties of polystrene (PS) latex/multi-walled Carbon nanotube (MWNT) composites. Films prepared from PS/MWNT mixtures with different MWNT content were separately annealed above glass transition temperature of PS. Film formation stages of PS/MWNT composites were followed by monitoring the change in transmitted light intensity, I_{tr}. The surface conductivity of films was found to increase dramatically above 4 wt% MWNT following the percolation theory. The conductivity scales with the mass fraction of MWNT as a power law with exponent 2.27, extremely close to the value of 2.0 predicted by percolation theory.

Keywords: PS Latex; Composite film; MWCNT;Conductivity; Photon Transmission;Percolation

1. INTRODUCTION

As a result of worldwide efforts by theorist and experimentalists, a very good understanding of the mechanisms of latex film formation has been achieved[1]. Traditionally, the film formation process of polymer latex is considered in terms of three sequential steps: (i) water evaporation and subsequent packing of polymer particles (ii) deformation of the particles and close contact between the particles (iii) coalescence of the deformed particles to form a homogeneous film[2] where macromolecules belonging to different particles mix by interdiffusion[3,4].

Recently, CNT/polymer nanocomposites have been widely investigated due to their remarkable mechanical[4], thermal[5], and electrical properties[6]. CNT have potential applications in many areas such as biosensors, conducting agent, field-effect transistor, and nanocomposites[7]. Polymeric or

* Corresponding author. Tel.:+90(212)2856603 ; fax: +90(212)2856386.
E-mail address: saziye@itu.edu.tr.

 doi:10.1016/j.proeng.2011.04.285

ceramic matrix of composites is usually considered as non-conductive material because of its extremely low electrical conductivity (in the order of 10^{-10}–10^{-15} S/m). Dispersing conductive materials into the nonconductive matrix can form conductive composites. The electrical conductivity of a composite is strongly dependent on the volume fraction of the conductive phase. At low volume fractions, the conductivity remains very close to the conductivity of the pure matrix. When a certain volume fraction is reached, the conductivity of the composite drastically increases by many orders of magnitude. The phenomenon is known as percolation and can be well explained by percolation theory. The electrical percolation threshold of conductive reinforcements embedded in an insulating matrix is sensitive to the geometrical shape of the conductive phase. The small size and large aspect ratio (length/diameter) are helpful to lower the percolation threshold[8]**.** Depending on the matrix, the processing technique, and the nanotube type used, percolation thresholds ranging from 0.001 wt% to more than 10 wt% have been reported[9,10]. Because carbon nanotubes have tremendously large aspect ratios (100–10,000), many researchers have observed exceptionally low electrical percolation thresholds[10]**.**

In the work reported here, we investigated the film formation behavior and electrical conductivity properties of polymer/CNTs depending on CNTs content using photon transmission technique and electrical conductivity measurements. Films were prepared by mixing PS latex with MWNTs particles in various compositions and annealing them at temperatures above glass transition temperature of PS. After each annealing step, the transmitted light intensity, I_{tr} was monitored to observe the film formation process. The increase in I_{tr} up to healing temperature, T_h and above T_h during annealing was explained by void closure and interdiffusion processes, respectively. From the measurements of electrical conductivities of the composites, the percolation threshold of conductivity was found to be as 4 wt% MWNT.

2. EXPERIMENT

2.1 materials

PS particles were produced via surfactant free emulsion polymerization process. The polymerization was performed batch-wisely using a thermostatted reactor equipped with a condenser, thermocouple, mechanical stirring paddle and nitrogen inlet. The agitation rate was 400 RPM and the polymerization temperature was controlled at 70 $^{\circ}$C. Water (100 ml) and styrene (5 g) were first mixed in polymerization reactor where the temperature was kept constant (at 70°C). Potassium peroxodisulfate (KPS) initiator (0.1g) dissolved in small amount of water (2ml) was then introduced in order to induce styrene polymerization. The polymerization was conducted during 18 hours. The polymer has a high glass transition temperature (T_g=105 ^{0}C). The latex dispersion has an average particle size of 400 nm.

Commercially available MWNTs (Cheap Tubes Inc., VT, USA, 10-30 μm long, average inner diameter 5-10 nm, outer diameter 20-30 nm, the density is approximately 2.1 g/cm^3 and purity higher than 95 wt %) were used as supplied in black powder form without further purification. A stock solution of MWNTs was prepared following the manifacturers regulations: nanotubes were dispersed in deionized (DI) water with the aid of Polyvinyl Pyrolidone (PVP) in the proportions of 10 parts MWNTs; 1-2 parts PVP; 2.000 parts DI water by bath sonication for 3h. PVP is a good stabilizing agent for dispersions of carbon nanotubes, enabling preparation of polystyrene composites from dispersions of MWNT in polystyrene solution.

2.2. Preparation of PS/MWNT composite films

A 15 g/L solution of polystyrene (PS) in water was prepared separately. The dispersion of MWNT in water was mixed with the solution of PS yielding the required ratio, R of MWNT in PS latex by using the relation $R = \frac{M_{MWNT}}{M_{PS} + M_{MWNT}}$. Each mixture was stirred for 1h followed by sonication for 30 min at room

temperature. By placing the same number of drops on a glass plates with similar surface areas (0.8x2.5 cm^2) and allowing the water to evaporate at 60 ^{0}C in the oven, dry films were obtained. After drying, samples were separately annealed above T_g of PS for 10 min at temperatures ranging from 100 to 270°C. The temperature was maintained within ±2°C during annealing. After each annealing step, films were removed from the oven and cooled down to room temperature. The thickness of the films was determined from the weight and the density of samples and ranges from 6 to 10 μm.

2.3 Measurements

Photon transmission experiments were carried out using model Carry 100 bio UV-Visible (UVV) spectrometer from Varian. The transmittances of the films were detected at 500 nm. A glass plate was used as a standard for all UVV experiments.

Scanning electron microscope (SEM) images were taken by using LEO Supra VP35 FESEM.

Electrical conductivity was measured by a two-probe method using a Keithley Model 6517a Electrometer with ultrahigh resistance meter. For the surface resistance measurements, the samples were coated onto thin rectangular glass slabs with typical dimensions 2.0x3.0 cm^2. The electrical contact was made using a silver paste. The surface resistivity was converted into surface conductivity.

3. RESULTS AND DISCUSSION

3.1 Film Formation Process of PS/MWNT Composites

I_{tr}, intensities versus annealing temperatures are plotted in Fig 1 for the films with 0, 1.5, 3, 5, 10, and 15 wt% MWNT content. Upon annealing the transmitted light intensity, I_{tr} started to increase for all film

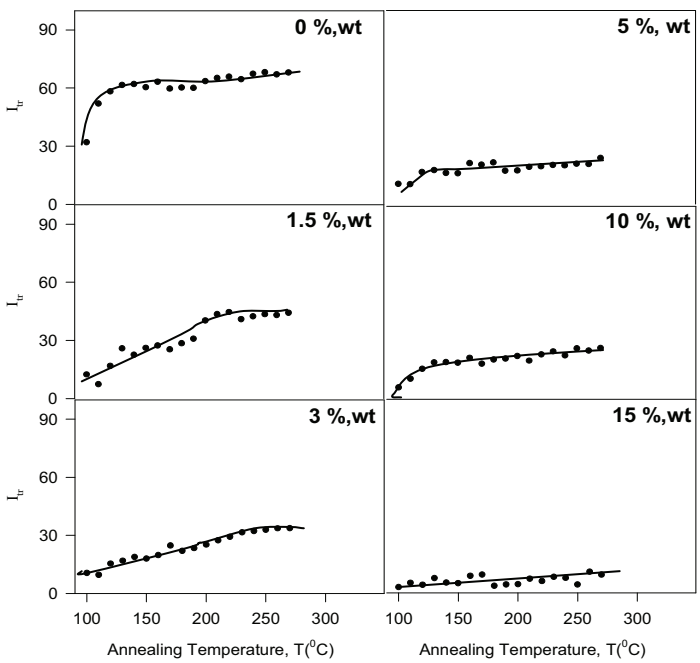

Fig 1. Plots of transmitted photon intensities, I_{tr} versus annealing temperatures depending on MWNT content in the films. Numbers on each figure shows the MWNT content in the film.

samples except for 15 wt% MWNT content film. The increase in I_{tr} with annealing can be explained by the evaluation of transparency of the films and surface smoothing upon annealing. Most probably increase in I_{tr} up to T_h (see Figure 3) corresponds to the void closure process[11-15], i.e. the polystyrene

starts to flow upon annealing and voids between particles can be filled. On the other hand, increase in I_{tr} above T_h corresponds the interdiffusion process. However, for 15 wt% MWNT content film, I_{tr} almost doesn't change with annealing which means that no film formation process occur, and light transmission is completely blocked by dispersion of MWNTs in the composite film. On the other hand, I_{tr} decreases with increasing MWNT content in films at all annealing temperatures, predicting less transparency occurs at high MWNT content films.

To see the dispersion of MWNTs in PS matrix, SEM micrographs of composite film with 15 wt% MWNT content were taken after annealing at different temperatures (see Fig 2). In Fig 2a, for the 15

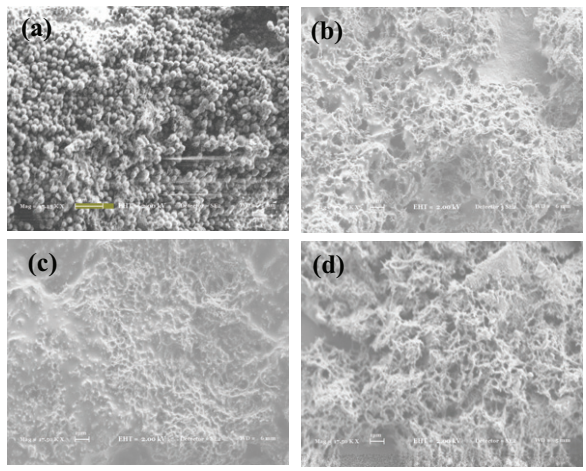

Fig 2. Scanning electron micrographs (SEM) of composite films prepared with 15% MWNT content and annealed for 10 min at **a-** 100, **b-** 150, **c-** 180 and **d-** 220 ^{0}C temperatures.

wt% MWNT film annealed at 100 ^{0}C no deformation in PS particles is observed and PS particles keep their original spherical shapes. After annealing treatment at 150, 180 and 220 ^{0}C (Fig 2c, d and e), SEM images show that complete particle coalescence has been achieved. It can be clearly seen that composite film consists of a network of bundles and indicates significant porosity which results strong scattering.

The increase in I_{tr} intensity below and above T_h point in the (0–10) wt% MWNT range (see Figure 3) can be explained by void closure and interdiffusion processes, respectively[16]. To understand these phenomena, the following mechanisms and their formulations are proposed.

3.1.1 Voids Closure

Latex deformation and void closure between particles can be induced by shearing stress which is generated by surface tension of polymer i.e. polymer-air interfacial tension. In order to relate the shrinkage of spherical void of radius, r to the viscosity of surrounding medium, η an expression was derived and given by the following relation[17].

$$\frac{dr}{dt} = -\frac{\gamma}{2\eta}\left(\frac{1}{\rho(r)}\right) \tag{1}$$

where γ is surface energy, t is time and $\rho(r)$ is the relative density. It has to be noted that here surface energy causes a decrease in void size and the term $\rho(r)$ varies with the micro structural characteristics of the material,

such as the number of voids, the initial particle size and packing. Using the Frenkel-Eyring theory for the temperature dependence of viscosity[18-20] and integrating Eq 1, the following equation is obtained:

$$t = -\frac{2A}{\gamma}\exp\left(\frac{\Delta H}{kT}\right)\int_{r_0}^{r}\rho(r)dr \tag{2}$$

Where A is a constant and ΔH is the activation energy of viscous flow i.e. the amount of heat which must be given to one mole of material for creating the act of a jump during viscous flow. Assuming that the interparticle voids are in equal size and number of voids stay constant during film formation (i.e. $\rho(r)\infty r^{-3}$), then integration of Eq 2 gives the relation

$$t = \frac{2AC}{\gamma}\exp(\frac{\Delta H}{kT})(\frac{1}{r^2} - \frac{1}{r_0^2}) \tag{3}$$

where, C is a constant related to relative density $\rho(r)$. In order to quantify the behavior of I_{tr} curves below T_h presented in Fig 3, void closure model can be applied, where decrease in void size (r) causes an increase in $I_{tr}/(I_{tr})_{max}$ ratios and vice versa. If the assumption is made that $I_{tr}/(I_{tr})_{max}$ ratio is inversely proportional to the 6th power of void radius, r then Eq 3 can be written as

$$t = \frac{2AC}{\gamma}\exp(\frac{\Delta H}{kT})(\frac{I_{tr}}{(I_{tr})_{\max}})^{1/3} \tag{4}$$

Here, r_0^{-2} is omitted from the relation since it is very small compared to r^{-2} values after a void closure process is started. Eq 4 can be solved for $I_{tr}/(I_{tr})_{max}$

$$I_{tr}(T) = S(t)\exp\left(-\frac{3\Delta H}{kT}\right) \tag{5}$$

where $S(t) = (yt/2AC)^3$, *and* $I_{tr}=I_{tr}/(I_{tr})_{max}$. For a given time the logarithmic form of Eq 5 can be written as follows

$$LnI_{tr}(T) = LnS(t) - (\frac{3\Delta H}{k_B T}) \tag{6}$$

3.1.2 Healing and Interdiffusion

The decrease in I_{tr} was already explained in the previous section, by the increase in transparency of latex film due to disappearing of deformed particle-particle interfaces. As the annealing temperature is increased above healing temperature, T_h, some part of the polymer chains may cross the junction surface and particle boundaries start to disappear, as a result I_{tr} increases due to the shorter optical and long mean free paths of a photon[12-16]. In order to quantify these results, the Prager-Tirrell (PT) model[21] for the chain crossing density can be employed. These authors used de Gennes's "reptation" model to explain configurational relaxation at the polymer-polymer junction where each polymer chain is considered to be confined to a tube in which executes a random back and forth motion. They calculated the total "crossing density" σ(t) (chains per unit area) at junction surface in terms of reduced time $\tau = 2vt/N^2$ as

$$\sigma(\tau)/\sigma(\infty) = 2\pi^{-1/2}\left[\tau^{1/2} + 2\sum_{k=0}^{\infty}(-1)^n\left[\tau^{1/2}\exp(-k^2/\tau) - \pi^{-1/2}erfc(k/\tau^{1/2})\right]\right] \tag{7}$$

For small τ values the summation term of the above equation is very small and can be neglected, which then results in

$$\sigma(\tau)/\sigma(\infty) = 2\pi^{-1/2}\tau^{1/2} \tag{8}$$

the temperature dependence of $\sigma(\tau)/\sigma(\infty)$ can be modeled by taking into account the following Arrhenius relation for the linear diffusion coefficient

$$\nu = \nu_o \exp(-\Delta E_b / kT) \tag{9}$$

Here ΔE_b is defined as the activation energy for backbone motion depending on the temperature interval. Combining Eq 8 and Eq 9 a useful relation is obtained as

$$\sigma(\tau)/\sigma(\infty) = A_o \exp(-\Delta E_b / 2kT) \tag{10}$$

where $A_o = (8\nu_o t / \pi N^2)^{1/2}$ is a temperature independent coefficient.

The increase in I_{tr} above T_h is already related to the disappearance of particle-particle interfaces i.e. as annealing temperature is increased, more chains relaxed across the junction surface and as a result the crossing density increases. Now, it can be assumed that I_{tr} is proportional to the crossing density $\sigma(\tau)$ in Eq. 10 and then the phenomenological equation can be written as

$$I_{tr}(T) / I_{tr}(\infty) = A \exp(-\Delta E / 2kT) \tag{11}$$

Logarithmic plots of I_{tr} vs. T^{-1} are presented in Fig 3 (left hand side of the curves) for various MWCNT content. The activation energies, ΔE are produced by least squares fitting the data to Eq 11 and are listed in Table 1, where it is seen that ΔE values present a maximum around 3 wt % MWNT content while ΔH

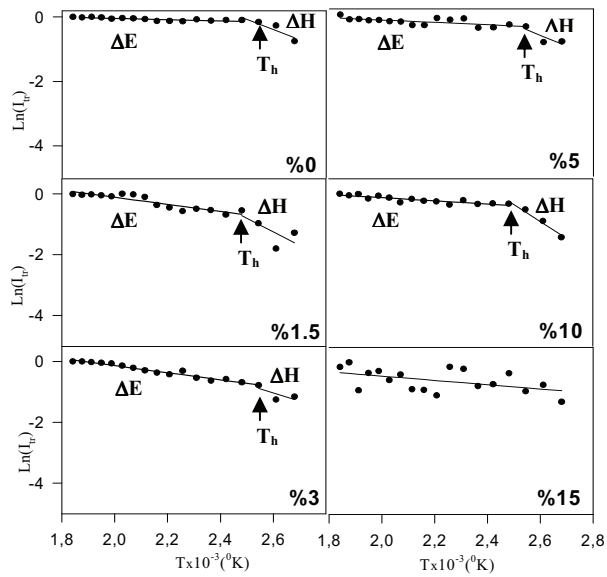

Fig 3. The $Ln(I_{tr})$ versus T^{-1} plots of the data in Fig 1. The slope of the straight lines produces ΔH and ΔE activation energies which are listed in table 1.

Table 1: Experimentally determined activation energy values.

MWNT (wt%)	0	1.5	2	3	4	5	10	15
ΔH (kcal/mol)	2.1	3.0	1.1	1.8	0.8	2.2	3.7	-
ΔE (kcal/mol)	0.7	4.6	8.6	4.6	5.5	1.4	2.1	-

values have a minimum about the same point. Another words interdiffusion of polymer chains needs more energy to cross over the junction surface than amount of heat which was required by one mole of polymeric material to accomplish a jump during viscous flow. In fact these optimum points correspond to the percolation threshold for the electrical conductivity and for the optical transparency in composite film (see next section).

3.2. Electrical Conductivity of PS/MWNT Composites

The surface conductivity properties of the films were measured at room temperature by using a two probe technique. Fig 4a shows the electrical conductivity (σ) of PS/MWNT composite films as a function of MWNTs ratio, *R*. While low MWNT content composites (R<0.04) show similar

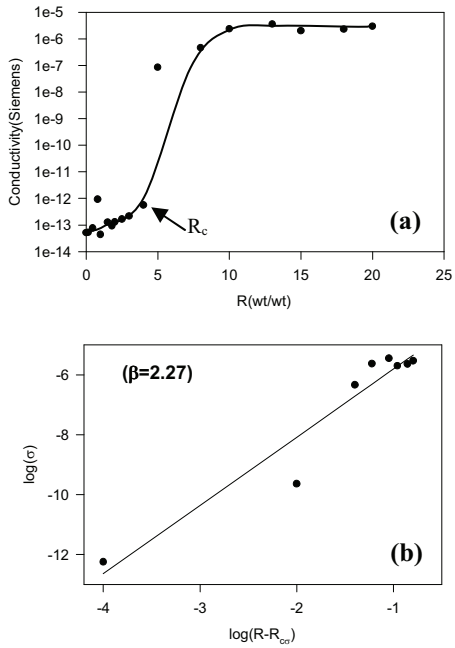

Fig 4. a) Conductivity, σ versus MWNT content, R (wt/wt) **b)** Log–Log plot of σ versus (R-R_c).

conductivity between 10^{-13}-10^{-12} S the conductivity of high MWNT content films (R>0.04) increase dramatically to ~10^{-7}-10^{-6} S. In other words, above 0.04 MWNTs form an interconnected percolative network. However, below 0.04 clusters of MWNT become separated by the polystyrene layers. From here we could conclude that the electrical conductivity of the films exhibited a type of percolation[22] behavior.

3.2.1. Percolation Theory

The basis of the percolation theory is to determine how a given set of sites, regularly or randomly positioned in some space, is interconnected[22]. At some critical probability, called the "percolation threshold (p_c)", a connected network of sites is formed which spans the sample, causing the system to percolate. Two types of percolation were considered: site percolation, where sites in a lattice are either filled or empty, or bond percolation, where all the sites in a lattice are occupied, but are either connected or not[23]. Extensive simulations and theoretical work have shown that the percolation probability, $P_\infty(p)$ vanishes as a power-law near p_c :

$$p_\infty(p) \approx (p - p_c)^\beta \tag{12}$$

For all volume fractions $p>p_c$, the probability of finding a spanning cluster extending from one side of the system to the other side is 1. The largest cluster spans the lattice connecting the left and right edges to the bottom edge, which is called "percolating cluster". Whereas for all volume fractions $p < p_c$, the probability of finding such an infinite cluster is 0.

The conductivity, σ of a percolative system is generally described as a function of mass fraction, R by the scaling law in the vicinity of the percolation threshold ($R_{c\sigma}$):

$$\sigma = \sigma_0 (R - R_{c\sigma})^{\beta_\sigma} \quad , \tag{13}$$

Where σ is composite conductivity (in Siemens), σ_0 is the self conductivity of MWNTs film and is equal to 1. R presents weight fraction of MWNTs, $R_{c\sigma}$ presents percolation threshold of conductivity and β_σ is

critical exponent. This equation is valid at concentrations above the percolation threshold, i.e., when $R > R_{c\sigma}$. The value of the critical exponents, β_σ, is dependent on the dimensions of the lattice[24].

In order to calculate the percolation threshold, Eq 13 was transformed into the logarithmic form:

$$\log(\sigma) = \log(\sigma_0) + \beta_\sigma log|R-R_c| \quad (14)$$

Then to produce an estimated value for $R_{c\sigma}$ and the critical exponent β_σ we fitted the $\log(\sigma)$-$log|R-R_c|$ data in Fig 4b for $R>R_{c\sigma}$ to Eq 14. The value of β_σ has been determined from the slope of the linear relation of $\log(\sigma)$-$log|R-R_c|$ plot on Fig 4b and found to be as 2.27. This value agrees well with the universal scaling value of β_σ=2.0. In three dimensional lattice systems[23] β_σ values change from 1.3 to 3. The fact that β_σ is not significantly greater than 2.0 also suggest that the bundles are not separated by polymer tunneling barriers, shows that the polymer coating observed in Fig 2 cannot simply coat individual bundles but must coat the network as whole, allowing intimate contact between bundles at junction sites.

4. CONCLUSION

We have reported an investigation of the film formation and electrical conductivity of PS/MWNT composites. Below 10 wt% MWNT content, two distinct film formation stages which are named as void closure and interdiffusion were observed. However, MWNT concentrations above 10 wt% MWNT no film formation can be achieved. On the other hand, sample conductivities were observed to depend strongly on the MWNT contents which are drastically changed with increase of the MWNT content above the percolation threshold of 4 wt% MWNT. With the introduction of 4 wt% MWNTs, the conductivity presented an increase by 7-6 orders of magnitude compared with low MWNT content films.

Void closure (ΔH) and interdiffusion (ΔE) activation energies presented optimum values around the threshold of the electrical contuctivity and optical transparency percolation around 4 wt% MWNT content. Our results are quite similar to other reports on low conductance with CNTs amount and start to saturate at higher CNTs content. Further investigation of electrical properties of the composite films is underway in our laboratory to understand the behaviors of (ΔH) and (ΔE) activation energies around the percolation point.

5. REFERENCES

[1]Provder T., Winnik M.A. and Urban M.W., *Film Formation in Waterborne Coatings* (Eds.), ACS Symp. , Amer. Chem. Soc. Ser., (1996), 648
[2]Mackenzie JK. Shuttleworth R., Proc. Phys. Soc. (1949); 62; 838.
[3]-Yoo J. N., Sperling L. H., Glinka C. J., Klein A., *Macromolecules,* (1991), 24, 2868.
[4]-Pekcan Ö., *Trends Polym. Sci.,* (1994), 2, 236.
[5]-Baughman R. H., Zakhidov A. A., de Heer W. A., *Science* (2002), *297*, 787.
[6]-Coleman J. N., Khan U., Blau W. J., Gun'ko Y. K., *Carbon* (2006), *44*, 1624.
[7]-Ajayan P.M., Zhou O.Z., "Applications of carbon nanotubes" Topics Apply. Phys., (2001) 80, 391-425,.
[8]-DM Bigg, Stutz DE. Plastic, Polym Compos (1983);4:40–6.
[9]-Grunlan JC et al. , Adv Mater (2004);16:150–3.
[10]-Kymakis E, Alexandou I, Amaratunga GAJ. , Synth Met (2002);127(1–3):59–62.
[11]-Du FM, Fischer JE, Winey KI. ,Phys Rev B (2005);72:121404.
[12]-Pekcan O. and Arda E., *Encyclopedia of Surface and Colloid Science,* Marcel and Dekker (2002), 2691
[13]-Pekcan O., Arda E., Bulmus V. and Piskin E., J. Appi. Polym. Sci. (2000), 77, 866.
[14]-Arda E., Ozer F., Piskin E. and Pekcan O., J. Coll. Interface Sci. (2001), 233, 271.
[15]-Arda E. and Pekcan Ö., Polymer (2001), 42, 7419.

[16]- Ugur S., Yargi Ö., Pekcan Ö. ,Composite Interface . (2008), 15, 4, 411–424.
[17]-Keddie J.L., Meredith P., Jones R.A.L and Donald A.M., *Film Formation in Waterborne Coatings,* Provder T., Winnik M.A. and Urban M.W., (Eds.), ACS Symp. , Amer. Chem. Soc.. Ser., (1996), 648, 332-348.
[18]-Vogel H., Phys. Z., (1925), 22, 645.
[19]-Fulcher G. S., J. Am. Ceram. Soc., (1925), 8, 339.
[20]-Frenkel J., J. Phys. USSR, (1945), 9, 385.
[21]- **a)-**Prager, S., Tirrell, M., ,J. Chem. Phys. (1981) 75, 5194–5198 **(b)-**Wool, R.P., Yuan, B.L., McGarel, O.J., ,J. Polym. Eng. Sci. (1989),29, 1340–1367.
[22]- D. Stauffer and A. Aharony, "Introduction to Percolation Theory" Taylor&Francis, London, 1994.
[23]-Sahimi M., Applications of Percolation Theory London: Taylor and Francis (1994).
[24]-Broadbent S. R., Hammersley J. M.; Proc. Camb. Phil. Soc. (1957), 53,629.